Three-dimensional Numerical Prediction on the Evolution of Nocturnal Thermal High (Tropical Night) in a Basin

Hyo Choi[1] and Jeong-Woo Kim[2]

[1] Dept. of Atmospheric Environmental Sciences, Kangnung National University, Kangnung, Kangwondo 210-702, Korea

[2] Dept. of Astronomy and Atmospheric Sciences, Yonsei University, Seoul 120-749, Korea

(Manuscript received 17 October, 1997)

Abstract

Numerical prediction of nocturnal thermal high in summer of the 1995 near Taegu city located in a basin has been carried out by a non-hydrostatic numerical model over complex terrain through one-way double nesting technique in the Z^* following coordinate system. Under the prevailing westerly winds, vertical turbulent fluxes of momentum and heat over mountains for daytime hours are quite strong with a large magnitude of more than $120W/m^2$, but a small one of $5W/m^2$ at the surface of the basin. Convective boundry layer (CBL) is developed with a thickness of about 600m over the ground in the lee side of Mt. Hyungje, and extends to the edge of inland at the interface of land and sea in the east. Sensible heat flux near the surface of the top of the mountain is $50W/m^2$, but its flux in the basin is almost zero. Convergence of sensible heat flux occurs from the ground surface toward the atmosphere in the lower layer, causing the layer over the mountain to be warmed up, but no convergence of the flux over the basin results from the significant mixing of air within the CBL. As horizontal transport of sensible heat flux from the top of the mountain toward over the basin results in the continuous accumulation of heat with time, enhancing air temperature at the surface of the basin, especially Taegu city to be higher than 39.3^0C.

Since latent heat fluxes are 270W/m^2 near the top of the mountain and 300W/m^2 along the slope of the mountain and the basin, evaporation of water vapor from the surface of the basin is much higher than one from the mountain and then, horizontal transport of latent heat flux is from the basin toward the mountain, showing relative humidity of 65 to 75% over the mountain to be much greater than 50% to 55% in the basin.

At night, sensible heat fluxes have negative values of -120W/m^2 along the slope near the top of the mountain and -50W/m^2 at the surface of the basin, which indicate gain of heat from the lower atmosphere. Nighttime radiative cooling produces a shallow nocturnal suface inversion layer with a thickness of about 100m, which is much lower than common surface inversion layer, and lifts extremely heated air masses for daytime hours, namely, a warm pool of 34^{0}C to be isolated over the ground surface in the basin. As heat transfer from the warm pool in the lower atmosphere toward the ground of the basin occurs, the air near the surface of the basin does not much cool down, resulting in the persistence of high temeprature at night, called nocturnal thermal high or tropical night. High relative humidity of 75% is found at the surface of the basin under the moderate wind, while slightly low relative humidity of 60% is along the eastern slope of the high mountain, due to adiabatic heating by the srong downslope wind. Air temperature near the surface of the basin with high moisture in the evening does not get lower than that during the day and the high temperature produces nocturnal warming situation.

1. Introduction

In the recent years, frequently nighttime warming such as tropical night has occurred in urban areas and its driving mechanism has not been solved for many different kinds of reasons (Choi and Chae, 1997). Andre and Mahrt (1981) and Broast and Wyngaard (1978) explained that during clear nights over a flat land, one can usually observe the progressive build up of a stably stratified layer next to the surface due to the ground surface cooling. Segal et al. (1988) discussed thermally induced circulations over a valley and ridge with a two-dimensional numerical model and emphasized the importance of topographical effects such as horizontal scale of topography. Kondo et al. (1989) indicated that on calm and cloudless days, more sensible heat had to be accumulated in the valley region than over the mountainous areas, in order that the amplitudes of the diurnal variations of atmospheric temperature and surface pressure were much larger at the bottom of a valley. Kuwagata, et al. (1990) stated the daytime planetry boundary layer heating process over complex terrain under fair and calm weather conditions and Whiteman (1990) investigated thermally

developed wind system in mountainous terrain through observation.

Not only orgraphic effects of topographical feature, but also sea-land breeze phenomena often control coastal atmospheric circulations and temperature fields (Choi and Choi, 1997; Choi, et al., 1996; McPherson, 1970; Plate, 1971; Raynor et al., 1979). Especially, in the coastal region, the dynamical effects of meso-scale mountains in the large scale numerical models of the atmosphere play an important role for atmospheric circulation over coastal complex terrain (Boer et al., 1984; Palmer et al., 1986; Satomura and Bougeault, 1992) and diurnal variations of wind and temperature induced by sea-land breeze also give a great influence upon heat process (Hsu, 1980, 1988; SethuRaman, 1982).

The primary purpose of this study is to explain the driving mechanism of the formation of tropical night in a basin and the secondary is to verify and to predict its development by using a numerical model over complex terrain.

2. Data Analysis and Numerical Method

The study area for tropical night phenomenon in a fine-mesh domain consists of complex terrain, characterized by high mountains in the west and relatively low mountains in the north and east, but by almost plain topographical feature or very low mountains in the south. Tae Bak mountains lie from south toward north along the eastern coast of Korean peninsula and take another branch mountains toward south-west off Tae Bak mountains in a coarse-mesh domain (Fig. 1). Especially, Taegu city is located in a basin, almost the central part of the fine mesh domain and is about 50 km away from the coast as shown in Fig. 2.

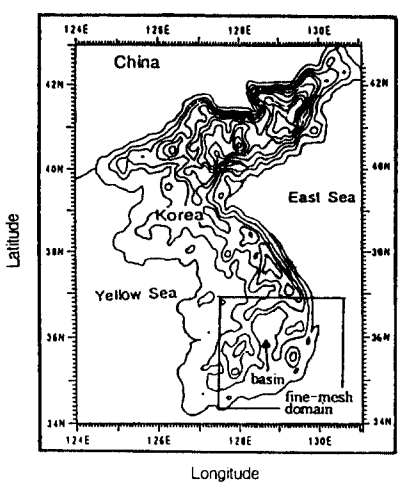

Fig. 1. Topographical feature of Korean peninsula and study area in a fine-mesh domain.

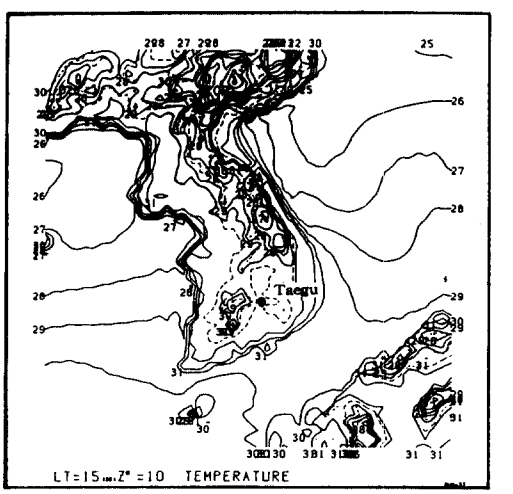

Fig. 2. Horizontal distribution of air temperature (^{0}C) surrounding Korean peninsula in a coarse-mesh domain near Korea at 1500 LST, August 14, 1995.

A non-hydrostatic grid point model in a complex terrain-following coordinate (x, y, z^*) was adopted to simulate evolution of tropical night in a basin for a 48 hour prediction experiment from 09 LST (Local Standard Time = 9h + Greenwith Mean Time), August 13 to 09 LST, August 15. The simulation was made by using HITACH super computer established at Meteorological Research Institute, Japan Meteorological Agency (JMA). The grid domain consists of 50 x 50 grid points with a uniform horizontal interval as 20 km in the coarse-mesh model and 5 km in the fine-mesh for one-way double nesting. This model has 15 vertical levels from 10 m over the ground surface to 6 km, that is, top of model domain, which are 10, 45, 120, 235, 350, 500, 700, 900, 1100, 1400, 1800, 2400, 3200, 4200 and 5400 m with sequentially a larger interval in the upper layers.

We horizontally and vertically interpolated 12 hourly global analysis data (G-ANAL) of atmospheric pressure, wind, potential temperature, specific humidity made by JMA for our two models with different resolutions, and the interpolated data were initially provided as lateral boundary data in a coarse-mesh model and then, predicted ones by the coarse-mesh model were treated as lateral boundary data in the fine-mesh model. For comparision of observed data on wind, air temperature, relative humidity with predicted ones by the numerical model, hourly based data measured by Korea Meteorological Administration were used.

Along the eastern Korean coastal region, the climate is usually modified by ocean currents which consist of North Korea Cold Current and East Korea Warm Current, and both atmospheric circulation and heat budget are also affected by these two different kinds of cold and warm water masses. Thus, the reanalyzed SST data from National Oceanic and Atmospheric Admistration(NOAA) satellite image picture were used in this study area (NFRDA, 1995).

3. Numerical Model Formulations

3.1 Basic equations

A non-hydrostatic and imcompressible model in a terrain-following coordinate system is based upon Boussinesq and anelastic approximations (Kimura and Arakawa, 1983; Kimura and Takahashi, 1991). The equations of motion for three components are composed as follow:

$$d_t hu = fhv - h\Theta\partial_x\pi' + \Theta(z_T - z^*)\partial_x z_G\partial_{z^*}\pi' + z_T^2/h\partial_{z^*}(K_m\partial_{z^*}u), \quad (1)$$

$$d_t hv = -fhu - h\Theta\partial_y\pi' + \Theta(z_T - z^*)\partial_y z_G\partial_{z^*}\pi' + z_T^2/h\partial_{z^*}(K_m\partial_{z^*}v), \quad (2)$$

$$d_t hw^* = -z_T\Theta\partial_{z^*}\pi' + gh\theta'/\Theta, \quad (3)$$

where z^* is the terrain-following vertical coordinate defined as

$$z^* = z_T(z - z_G)/h,$$

$$h = z_T - z_G ,$$

$$d_t = \partial_t + u\partial_x + v\partial_y + \dot{w}\partial_{z^*},$$

$$h\dot{w} = z_T w + (z^* - z_T)(\partial_x z_G u + \partial_y z_G v),$$

and

$$\theta = T(P_{00}/P)^{R/C_p}, \tag{4}$$

$$\theta' = \theta - \Theta,$$

$$\pi = (P/P_{00})^{R/C_p}, \tag{5}$$

$$\pi' = \pi - \pi_h.$$

Here π, Θ, θ, T, K_m, g, z, z_G and z_T are atmosphereic pressure at a given level, mean potential temperature of whole atmosphere in the model domain, potential temperature, air temperature at a level, vertical diffusion coefficient for turbulent momentum (m^2/s), gravity (m/s^2), actual height and height of ground surface above sea level and height of the upper boundary of the model atmosphere, respectively. f, P, P_{00}, R and C_p are Coriolis parameter ($= 2\Omega\sin\varphi$, Ω; angular velocity of the earth rotation, φ; latitude), atmospheric pressure, atmospheric pressure at reference level, gas constant for dry air and specific heat at constant pressure ($= 1.005 \times 10^3$ J/kg/K).

Radiative heating of air from both thermodynamic equation and conservation of water vapor may be written as

$$d_t h\Theta = z_T^2/h\partial_{z^*}(K_h\partial_{z^*}\Theta) + hQ_r. \tag{6}$$

$$d_t hq = z_T^2/h\partial_{z^*}(K_h\partial_{z^*}q), \tag{7}$$

where K_h, Q_r and q are vertical diffusion coefficient for turbulent heat, radiative heating or cooling rate of atmosphere and specific humidity of water vapor. The equation of continuity is given by

$$\partial_x hu + \partial_y hv + \partial_{z^*}h\dot{w} = 0. \tag{8}$$

As horizontal scale of the phenomena, in general, is one order greater than vertical scale, pressure equations from Eq.(3) for hydrostatic equilibrum state can be derived as

$$\partial_{z^*}\pi' = h/z_T,\ g/\Theta^2,\theta' \tag{9}$$

and for non-hydrostatic one

$$\partial_{z^*}\pi_h = gh\theta/(\Theta^2 z_T), \tag{10}$$

$$\begin{aligned}&\partial_{xx}\pi' + \partial_{yy}\pi' + \{(z_T/(z_T - z_G))^2\\ &+ ((z^* - z_T)/h)^2\,((\partial_x z_G)^2 + (\partial_y z_G)^2)\}\partial_{z^*z^*}\pi'\\ &+ 2(z^* - z_T)/h\;\partial_x z_G\;\partial_{xz^*}\pi' + 2(z^* - z_T)/h\;\partial_y z_G\;\partial_{yz^*}\pi'\\ &+ \{(z^* - z_T)/h\;(\partial_{xx}z_G + \partial_{yy}z_G)\\ &+ 2(z^* - z_T)/h^2\,((\partial_x z_G)^2 + (\partial_y z_G)^2)\}\partial_{z^*}\pi'\\ &= r(x, y, z^*)/(\Theta h),\end{aligned} \tag{11}$$

where r is written by

$$\begin{aligned}r(x, y, z^*) = {}&\partial_x ADVX + \partial_y ADVY + z_T/h\;\partial_{z^*}ADVZ\\ &+ 1/h\;\partial_x z_G\partial_{z^*}(z^* - z_T)ADVX\\ &+ 1/h\;\partial_y z_G\partial_{z^*}(z^* - z_T)ADVY,\end{aligned} \tag{12}$$

and

$$\begin{aligned}ADVX = {}&-\partial_x huu - \partial_y huv - \partial_{z^*}huw^* + fhv\\ &- \Theta h\partial_x\pi' - \Theta(z^* - z_T)\partial_x z_G\,\partial_{z^*}\pi'\\ &+ z_T^2/h\partial_{z^*}(K_m\partial_{z^*}u),\end{aligned}$$

$$\begin{aligned}ADVY = {}&-\partial_x huv - \partial_y hvv - \partial_{z^*}hvw^* - fhu\\ &- \Theta h\partial_y\pi' - \Theta(z^* - z_T)\partial_y z_G\,\partial_{z^*}\pi'\\ &+ z_T^2/h\partial_{z^*}(K_m\partial_{z^*}v),\end{aligned}$$

$$ADVZ = -\partial_x huw - \partial_y hvw - \partial_{z^*}hww^*.$$

For solving Eqs. (1), (2), (6) and (7), Euler-backward scheme was adopted for time integration and Crank-Nicholson scheme was for vertical direction in z^* coordinate. The atmospheric pressure changes at the top of model atmosphere with a material surface were controlled by wave radiation condition suggested by Klemp and Durran (1983), in order to avoid reflections of gravity waves generated by the local circulations in the lower layers. Periodic lateral boundary condition developed by Orlanski (1976) was applied to the calculation of u, v, θ and q in our model domain. In our numerical simulation, a large time interval, $\Delta t = 20$ sec in the coarse-mesh model and a small time interval, $\Delta t = 10$ sec in the fine-mesh model are determined to effectively reduce external gravity waves appeared in the equations, especially for the non-hydrostatic model.

3.2 Vertical diffusion coefficients for turbulent momentum and heat

In the surface boundary layer, the vertical diffusion coefficients for turbulent momentum, K_m and heat, K_h were estimated by the turbulent closure level-2 model (Mellor and Yamada, 1974; Yamada, 1983; Yamada and Mellor, 1983). As omitting upper subsripts of z and θ', the diffusion coefficients are

$$K_m = \ell e S_m,$$
$$K_h = \ell e S_h, \tag{13}$$

and

$$\ell = kz/(1 + \ell_o/kz),$$
$$\ell_o = 0.1 \int ezdz / \int edz,$$
$$e^2 = B_1 \ell^2 \{S_m (z_T/h)^2 \{(\partial_z u)^2 + (\partial_z v)^2\} - g/\Theta . S_h (z_T/h) \partial_z \theta\},$$
$$B_1 = 16.6,$$

where k and B_1 are von Karman's constant (≈ 0.4) and closure constant. The turbulent length, ℓ, is diagnostically determined to be smaller than a mixing length and turbulent velocity, e^2 (= $(e^2)^{1/2}$) is evaluated by considering the balance between production and dissipation of turbulent energy due to shear and buoyancy.

From the relation between stability factors, S_m, S_h and flux Richardson number, R_f semi-empirical formulae is given by

$$S_m = 1.76 (0.1912 - R_f)(0.2341 - R_f)/\{(1 - R_f)(0.2231 - R_f)\}$$
$$= 0.085, \quad \text{for } R_f \geq 0.16,$$

$$S_h = 1.318 (0.2231 - R_f)/(0.2341 - R_f) S_m$$
$$= 0.095, \quad \text{for } R_f \geq 0.16, \tag{14}$$

where R_f at each grid point can be evaluated by bulk Richardson number, R_i as

$$R_f = 0.6588 (R_i + 0.1776 - (R_i^2 - 0.3221 R_i + 0.03156)^{1/2}),$$
$$\text{for } R_i \leq 0.19,$$

$$R_i = g/\Theta . \partial_z \theta / (\partial_z U)^2, \tag{15}$$

and K_m and K_h are computed from the values of $U(=(u^2 + v^2)^{1/2})$ and θ in the staggared grid system between upper and lower levels of the model domain.

3.3. Long wave radition

Total net flux of long wave radiation, R_g, absorbed by water vapor and carbon dioxide is defined by

$$R_g = \sigma T_c^4 \tau_c + \sigma(T_{oo}^4 - T_c^4)\,\tau_f(U_{oo}) + \sum \sigma(T_i^4 - T_{i+1}^4)\,\tau_f(|U_i|), \tag{16}$$

where

$$\begin{aligned} &T_c = 200K, \\ &\tau_f = \tau_{H2O} \cdot \tau_{C02}, \\ &\tau_{H2O} = (1 + 1.746U^{\cdot 0.423})^{-1}, \\ &\tau_{C02} = 0.93 - 0.066LOG_{10}(U^{\cdot}_{C02}), \\ &\tau_c = (1 + 3.0U^{\cdot 0.408})^{-1} \cdot \tau_{C02}, \\ &U^{\cdot} = 1/g \int q(p/p_o)^{0.6} dp, \\ &U^{\cdot}_{C02} = (p_o^2 - p^2)/p_o^2. \end{aligned} \tag{17}$$

Here flux from the ground surface toward the upper levels is assumed to have a positive sign. σ, τ_f, T_c, T_{oo} and T_i are Stefan-Boltzman constant (= $5.67 \times 10^{-8} W/m^2/K^4$), transmission function, critical temperature (= 220K), temperature at the top of model atmosphere and temperature at the i-th level, respectively. τ_{H20} and τ_{C02} imply H_2O and CO_2 transmission fuctions. $U^{\cdot}$, q, p_o and p are effective vapor amount, specific humidity (g/cm^2), pressure (mb) at the surface and at an arbitary level, respectively.

Radiative heating rate of atmosphere with time, Q_r can be approximated by considering Newtonian cooling due to long wave radiation for air (T) and soil temperatures (T_g) at the ground surface.

$$Q_r = 10^{-5}(T_g - T), \qquad \text{for } T > T_g, \tag{18}$$

$$Q_r = 0, \qquad \text{for } T \leq T_g. \tag{19}$$

3.4 Solar radiation

Solar radiation toward the earth surface, which has a positive flux and total net solar radiation, S_g at the ground yields to

$$S_g = (1-\alpha_s)\{S_{os}(1 - \alpha_A)/(1 - \alpha_A \alpha_s) + S_{oA}(1 - A(x))\},$$

where

$$
\begin{aligned}
&S_{os} = 0.651\ S_o \cos\zeta, \\
&S_{oA} = 0.349\ S_o \cos\zeta, \\
&\cos\zeta = \cos\varphi \cos\delta \cosh + \sin\varphi \sin\delta, \\
&\alpha_A = 0.085 - 0.247\ \mathrm{LOG}_{10}\ (p/p_o \sec\zeta), \\
&x = U_T \sec\zeta, \\
&A(x) = 0.273x^{0.303}.
\end{aligned}
\tag{20}
$$

and S_o is solar constant, and S_{os} and S_{oA} imply scattering part of solar radiation ($\lambda<0.9\mu$) and absorption one ($\lambda>0.9\mu$). ζ is the solar zenth angle, which is a function of latitude(φ), the sun declination (δ) and the sun's hour angle (h). α_s and α_A are albedos of atmosphere and earth surface, and A(x) is an absorbing function of solar radiation by water vapor due to Rayleigh scattering.

3.5 Energy budget in the surface boundary layer

A constant flux layer is assumed to be below the lowest level of the model in the surface boundary layer such as $z^* = 10$ m height over the ground, and thus, similarity theory is applied to parameterize vertical turbulence. Momentum flux, τ, sensible heat flux, H and latent heat flux, H_L are expressed as

$$
\begin{aligned}
\tau &= -\rho (u_\cdot)^2 \\
&= -\rho k^2 |u^2| / \phi_m^2,
\end{aligned}
$$

$$
\begin{aligned}
H &= -\rho C_p \theta_\cdot u_\cdot \\
&= -\rho C_p k^2 |u| (\theta_1 - \theta_g)/(\phi_m \phi_h),
\end{aligned}
\tag{21}
$$

$$
\begin{aligned}
H_L &= -\rho L_e q_\cdot u_\cdot \\
&= -\rho L_e k^2 |u| (q_1 - q_g)/(\phi_m \phi_h),
\end{aligned}
$$

where ρ is the air density, $q_\cdot$ the water vapor scale or specific humidity scale, $u_\cdot$ the friction velocity, $\theta_\cdot$ the potential temperature scale, L_e the latent heat of vaporization. θ_1 and q_1 are potential temperature and specific humidity at the lowest level on the vertical grid points in the model atmosphere, and q_g and θ_g at the ground surface, respectively.

The integrated universal functions, ϕ_m for momentum and ϕ_h for heat are given by

$$
\begin{aligned}
\phi_m &= \int \Phi_m/\zeta \, d\zeta, \\
\phi_h &= \int \Phi_h/\zeta \, d\zeta,
\end{aligned}
\tag{22}
$$

here $\zeta = z/L$ and L is Monin-Obukhov length scale defined as

$$L = \rho C_p \theta u_*^3/kgH. \tag{23}$$

The following formulae suggested by Kimura and Takahashi (1991) are applied for the values of Φ_m and Φ_h, depending upon the atmospheric stability. For unstable condition,

$$\begin{aligned} \Phi_m &= (1 - 16\zeta)^{-1/4}, \\ \Phi_h &= (1 - 16\zeta)^{-1/2}, \qquad \text{for } \zeta \leq 0. \end{aligned} \tag{24}$$

For stable condition, we consider two classifications as

$$\begin{aligned} \Phi_m &= 1 + 7\zeta, \\ \Phi_h &= 1 + 7\zeta, \qquad \text{for } 0 < \zeta \leq \zeta_o. \end{aligned} \tag{25}$$

and

$$\begin{aligned} \Phi_m &= 1 + 7\zeta_o, \\ \Phi_h &= 1 + 7\zeta_o, \qquad \text{for } \zeta_o < \zeta. \end{aligned} \tag{26}$$

where

$$\begin{aligned} \zeta_o &= z_o/L = 0.714, \\ \zeta &= R_i \phi_m^2/\phi_h, \\ R_i &= g/\Theta(\theta_1 - \theta_g)\Delta z_1/|u|^2. \end{aligned}$$

Here Δz_1 and u are the depth of the lowest level from the ground surface and wind speed.

3.6 Soil temperaure at the ground surface

At the soil surface, a force restore method suggested by Deardorff (1978) is employed to estimate temporal change of potential temperature of the soil for bare ground condition, that is, change in the heat storage of the layer as follows:

$$\partial_t \theta_g = (S_g - R_g - H - H_L)/C_1 - (\theta_g - \theta_o)/C_2, \tag{27}$$

where

$$\begin{aligned} C_1 &= 0.5\ (\tau_d C_g k_g/2\pi)^{1/2}, \\ C_2 &= \tau_d/2\pi, \end{aligned}$$

$C_g = 0.2(1 + w_g)$,
$k_g = (0.386 + 0.15w_g) \times 10^{-2}$,

and S_g, R_g, θ_g and θ_o are radiative solar energy, longwave radiation, potentail temperatures of ground surface and underground, respectively. The coefficients, C_1 and C_2 can be evaluated by diurnal period, τ_d (= 24^h), heat capacity of underground soil, C_g (cal/cm^3/K) and heat conductivity, k_g (cal/cm/K/sec). Wetness of bare ground, w_g, which is defined as the ratio of available water content to maximum available water content and is treated as 0.2cal/cm^3/K for the summer time, similar to Kimura and Takahashi (1991).

Assuming that evaporation coefficient, B_g at the ground is constant such as $B_g = \min(1, 2w_g)$, specific humidity at the ground surface, q_g with a function of the soil temperature can be derived as

$$q_g = B_g\, q_s(T_g) + (1 - B_g)q_1, \quad \text{for } q_s(T_g) \geq q_1,$$

$$q_g = q_s(T_g), \quad \text{for } q_s(T_g) < q_1. \tag{28}$$

The concept of energy flux convergence or divergence and its relation to cooling or warming of a layer of the atmosphere or submedium has been explained. We discuss the significance of net flux convergence and divergence to warming or cooling in the lowest layer of the atmosphere, namely, planetry boundary layer. The rate of warming or cooling of a layer of air due to change of net radiation with height can be calculated from the principle of conservation of energy, as shown in equations (6), (7), (18) and (19).

4. Result and Discussion

4.1 Horizontal distribution of temperature and wind fields

In the afternoon on August 14, 1995, Taegu city was in the highest air temperature of 39.5^{0}C among the last 20 years' observation data and remained near 30^{0}C at night, under the persistence of nocturnal thermal high, called tropical night. First of all, temperature field and wind pattern around Korean peninsula in a coarse-mesh domain were investigated to find their influences upon the generation of tropical night in a local area.

The present numerical simulation shows that the general distribution of air temperatures depicts high temepratures in the Korean peninsula and south-eastern coastal regions including Taegu city were in a high temperature of 31^{0}C, as well (Fig. 2). Even if the general aspects of high air temperatures are found in the Korean peninsula, this computation result does not precisely reflect the real air temperature near Taegu city in a local specific area, showing a little bit lower temperature than the observed one at that time.

In a coarse-mesh domain, such kind of problem is usually caused by less effects of topography, that is, less orographic effect by lower height of the mountain and by less reflection of heat budget over complex terrain, due to automatically smoothing out those values in a wide horizontal grid interval of 20 km. On the other hand, during a one-way nesting process from a coarse-mesh domain to a fine-mesh domain, the numerical simulation in a fine-mesh domain can produce a temperature of 39.3^{0}C, very close to the observed one of 39.5^{0}C, under reconsideration of more accurate topographical feature in a small grid interval of 5km and predicated values of heat and moisture contents by the coarse-mesh model, as shown in Fig. 5a, later.

During the day, in the coarse domain, synoptic scale westerly winds at 10 m height over the ground surface prevail over the Yellow Sea and penerate into the Korean peninsula, passing through eastern coastal mountain regions (Fig. 3a). At this time, near the eastern coastal sea from Ulchin city (37^{0}N) to Vladivostok (41^{0}N), easterly winds are blowing from sea into inland sites, while southerly winds exist along the coast below Ulchin city to Pusan city (35^{0}N). In the open sea (the East Sea or the Sea of Japan), winds are, in general, southerly.

As Taegu city in an inland basin of south-eastern part of the Korean peninsula is under the influence of south-westerly winds, it is not directly affected by advection of moisture or

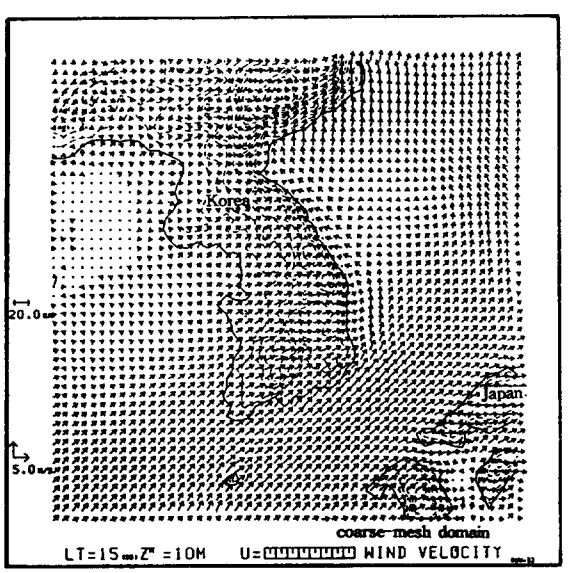

Fig. 3a. As shown in Fig. 2 except for horizontal wind field (m/s).

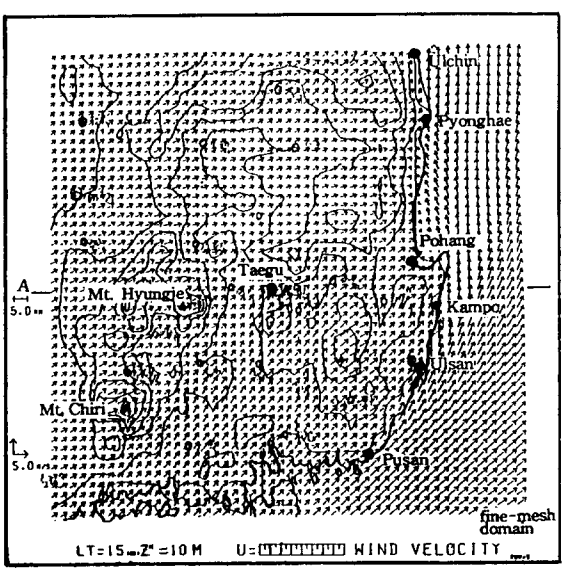

Fig. 3b. Horizontal wind field (m/s) in a fine-mesh domain near Taegu city at 1500 LST, August 14, 1995.

heat induced by a common sea breeze circulation from coastal sea in the east toward inland in the west, as shown in Fig. 3b.

As shown in Fig. 3b, in a fine-mesh domain, winds at 1500 LST near Taegu city, which consists of a basin with surrounding mountains in the west, north and east directions are south-westerly under the influence of the downslope of high mountains. More detail information of wind resume is found in Fig. 4a and 4b, which describe vertical profiles of winds on a straight cutting line (A-B) of Mt. Hyungje (west) - Taegu city - Kampo (east).

Since the synoptic westerly wind, during the day, suppresses meso easterly sea breeze from sea into inland, caused by horizontal temperature contrast between over inland surface and sea, resultant westerly wind speeds over the top of Mt. Hyungje and on its lee side slope, that is, eastern slope, are in the range of 4m/s to 5m/s and the surface wind speed in the basin is also 4m/s. Thus, the daytime westerly wind interrupted by the easterly sea breeze is localized with a moderate speed and is weaker than the wind at the starting time of sea breeze in the early morning.

As expected, the wind in the basin in the cross-sectonal area of the x-z coordinate for the daytime hours must be modified by both prevailing synoptic scale westerly wind blowing over the mountain and thermally induced upslope flow from the basin toward the mountain generated by the different thermal heating between the mountain slope and the basin rather than the sea breeze circulation.

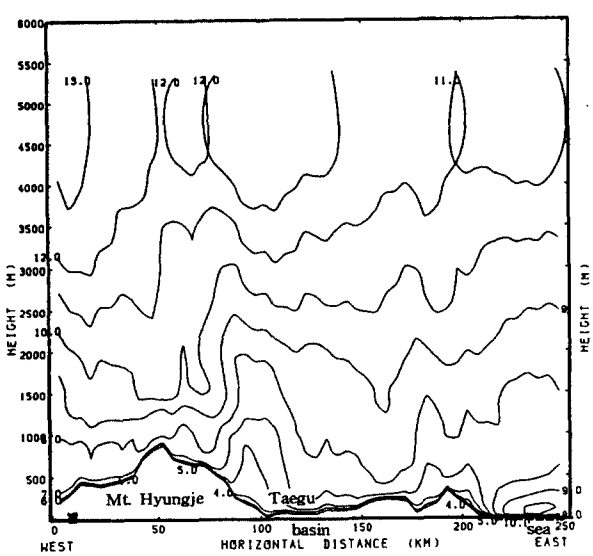

Fig. 4a. Veritcal profile of wind (m/s)on a straight cutting line (A-b):Mt. Hyungje (west)-Taegu-Kampo (east) in a fine-mesh domain as shown in Fig. 3b at 1500 LST, August 14, 1995.

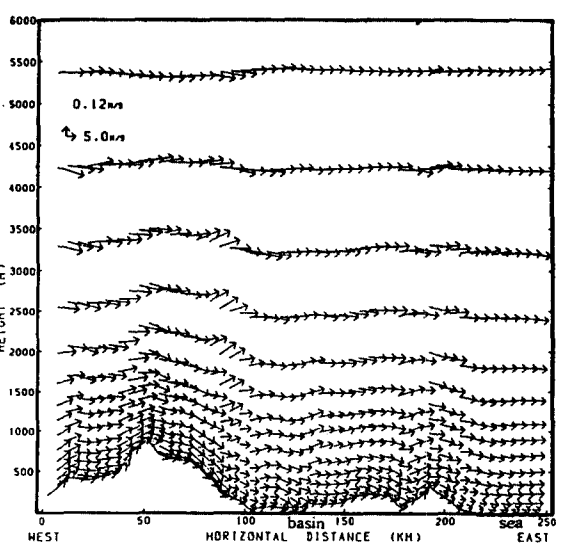

Fig. 4b. As shown in Fig. 4a, except for wind vector (m/s).

4.2 Thermal forcing over complex terrain

In Fig. 5a, it is necessary to investigate the reason why the high surface temperature could be produced in the basin, especially 39.5^{0}C at Taegu city. Fig. 5b shows vertical profiles of potential temperature deviation (θ') with solid lines, which indicate a stable state of the atmosphere. Convective boundary layer (CBL) is found to be under the development with a thickness of about 600 m over the windward and lee side ground surfaces of Mt. Hyungje and extends to the eastern edge of inland, which is an interface of land and coastal sea. In general, below a 1500 m height over the ground (θ' = 0 line), a deep convective boundary layer is detected in the land and relatively a shallow boundary layer with a thickness less than 200 m over the gound at the eastern coast.

Under this circumstance, Taegu city in the basin is in neutral atmospheric state, as shown with a vertical straight line of potential temperature deviation, which implys occurrence of vertical turbulent mixing or a mixed layer, but the heated air over the ground surface of the mountain becomes unstable over Mt. Hyungje in the left hand side of the model domain and over foothill or low mountains in the right side except for Taegu city. It is easily expected that there may be two kinds of thermal circulations in the left and right hand sides of Taegu city.

In order to verify existence of the thermal circulation, in detail, further consideration is given to turbulent fluxes of momentum and heat such as vertical diffusion coefficients for turbulent moment (K_m) and heat (K_h), which can easily estimate vertical motion of air due

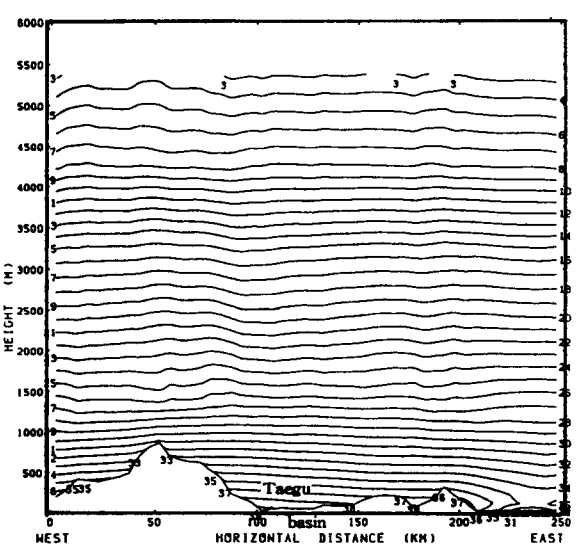

Fig. 5a. As shown in Fig. 4a, except for air temperature (^{0}C).

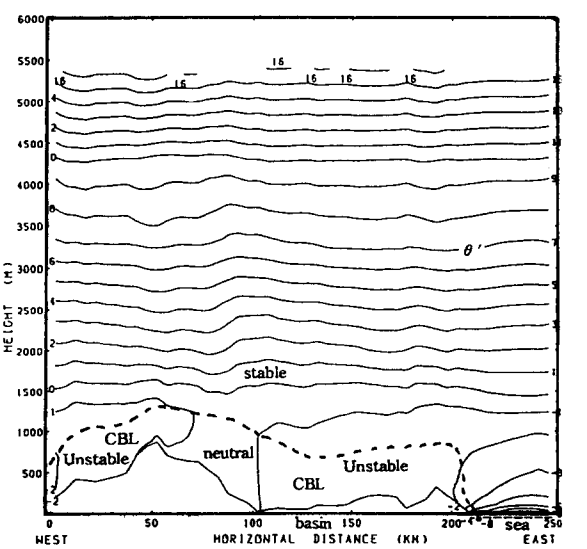

Fig. 5b. As shown in Fig. 4a, except for potential temperature deviation (K).

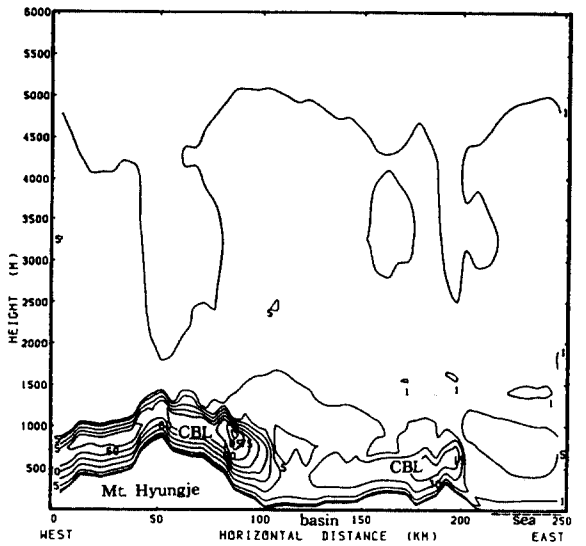

Fig. 6a. As shown in Fig. 4a, except for vertical diffusion coefficient for turbulent momentum (W/m^2).

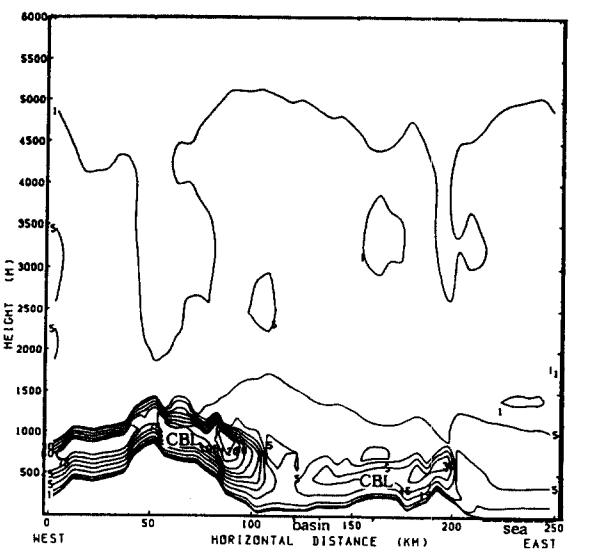

Fig. 6b. As shown in Fig. 4a, except for vertical diffusion coefficient for turbulent heat (W/m^2).

to daytime heat process (Fig. 6a). Along the slopes of two mountains, higher values of the diffusion coefficients are found over the mountain than the basin and are from a result of great diabatic heating over the mountain. In the upper atmospheric layer above 1500 m height, the turbulent heat diffusivity is almost constant and the development of the CBL is confined to this level.

At 1500 LST, their intensities in the lower atmosphere near the ground surface are quite strong with a magnitude of more than 100 W/m^2 for turbulent momentum and 120 W/m^2 for heat over Mt. Hyungje, and the thickness of the CBL is about 600 m above the mountain surface. Similarly, the diffusion coefficients of 30 W/m^2 and 45 W/m^2 are found over the top of the low mountain in the right hand side, producing almost the same thickness over the ground surface. On the other hand, low magnitudes of 5 W/m^2 and 1 W/m^2 are also detected near Taegu city in the basin and over the sea (Fig. 6b). However, even if their magnitudes are low near the ground surface of Taegu city, due to turbulrnt mixing of air, heating process is still expected to be continued in the basin. Thus, the thermally induced cross-valley circulation by upslope thermal flow along the slopes plays a role in the heat transport from the mountainous regions to the central part of the valley, namely, basin and lasts until the late afternoon.

Under the greater heating in the mountain range than in the basin, upslope winds induced by thermal forcing at the mountain surface are apparently well developed and converge toward the mountain ridge. In our case, the relatively strong synoptic westerly wind blowing over Mt. Hyungje suppresses the upslope thermal wind moving along the eastern slope of the mountain and resultant wind is still moderate westerly with no

circulation, at all, even if one can see a quite distinctive existence of two thermal ciculations from basin to two mountains in the west and east of the basin, under a weak wind. During the development of the CBL, mixing heights of air parcels are also vertically streched out and a mixed layer exists up to the height of 1500m above the surface of the basin.

The energy balance at the soil surface can be calculated by equations in sections 3-2 to 3-6. During the daytime, the surface receives radiative energy, so that it must give out heat to one or both of the media such as atmosphere and soil. Near the soil surface layer, an energy balance for daytime hours is achieved among the downward solar radiation, upward longwave radiation, sensible and latent heat fluxes and the heat flux into the soil. Namely, H (sensible heat flux) and H_L (latent heat flux) are typically all positive over land surfaces during the day.

As disscussed earlier, energy storage can be interpreted as the difference between the energy coming in and the energy goint out of the layer. When the energy input to the layer exceeds the outgoing energy, there is a flux convergence which results in the warming of the layer (Arya, 1988). On the other hand, when energy going out exceeds that coming in, the layer cools as a result of flux divergence.

At 1200 LST, sensible heat fluxes are 120 W/m^2 near the top of Mt. Hyungje on the left side of the basin and 70 W/m^2 over the low mountain on the right, where heat conductions are from the mountain surface toward the lower atmosphere, but the flux near the basin surface, especially, Taegu city is relatively a small magnitude of 50 W/m^2. Sensible and latent heat fluxes greatly depend upon location such as mountain, valley and sea, and the sensible heat flux in the basin surface is smaller than that over the mountain surface, especially top of Mt. Hyungje. At 1500 LST, when the highest temperature from observation data is detected at Taegu city in the basin, the sensible heat fluxes are 50 W/m^2, 0 W/m^2 and 10 W/m^2 at the surfaces of the high mountain, basin and low mountain, respectively (Fig. 7a).

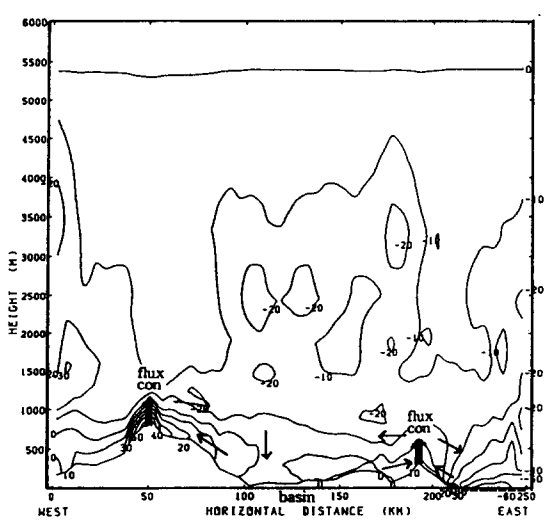

Fig. 7a. As shown in Fig. 4a, except for sensible heat flux (W/m^2).

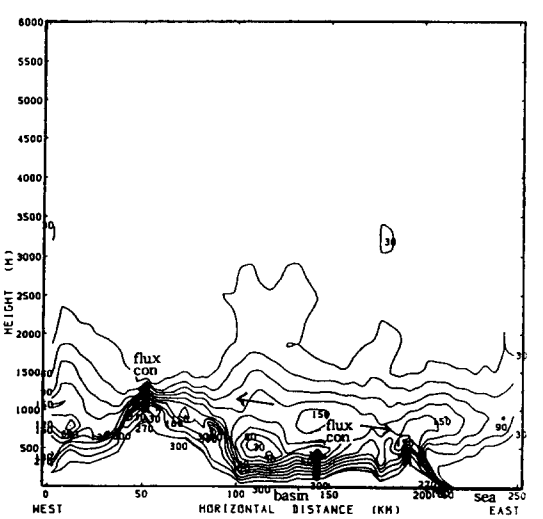

Fig. 7b. As shown in Fig. 4a, except for latent heat flux (W/m^2).

From Fig. 7a, the significance of sensible heat flux convergence takes a place in the lower layer of atmosphere over the top of the mountain, causing warming up of the layer. The difference between sensible heat fluxes over the mountain and basin can induce horizontal transport of sensible heat flux toward the lower atmosphere over basin and thus, a thermally induced local circulation can be generated by this transport. These processes of vertical flux convergence of sensible and latent heats and divergence are schematically shown in Fig. 7a and 7b. So, the downward motion of horizontally transported sensible heat flux from the mountain toward the lower atmospheric layer over the basin can accumulate some amounts of sensible heats near the surface of the basin, which are associated with a small magnitude of upward sensible heat flux from the surface of the basin or no upward flux at this time, resulting in well mixing of air parcels and showing reduced magnitudes of 0 W/m^2 of sensible heat flux over the basin and 50 W/m^2 over the mountain. Thus, more accumulation of sensible heat flux in basin by the horizontal transport than over mountainous area can make a great contribution to the formation of unusual highest air temperature of 39.5^0C at Taegu city.

However, when we only consider thermal forcing in the mountain and valley under no wind or weak wind, the wind in the upper part of thermal circulation over the mountain may be toward the basin and be opposite to the wind toward the mountain in the lower layer near the surface. Since originally existed strong westerly wind blowing over the mountain interrupts the movemnet of this thermal upslope flow along the eastern slope, resultant winds are westly with speeds of 5 m/s on the top of the mountain and 3 m/s or 4 m/s near the surface of the basin. They are much weaker than ones of 10m/s at the top of the mountain and 4 m/s, at 0900 LST before much developement of the convective boundary layer. Namely, as daytime goes on and the convective boundry layer continues to develop, upslope wind toward the top of the mountain is generated by the thermal circulation due to the difference of sensible heat fluxes over the slope of mountain and over the basin, but in our case, the prevailing strong westerly wind of 10 m/s along the eastern slope of the high mountain suppresses the thermally induced upslope wind, causing only westerly moderate wind in the model domain and showing no thermal circulation. Consequently, shortly after warming up of the lower atmosphere produced by vertical convergence of sensible heat flux over the top of mountain, the horizontal heat flux is easily transported from the mountain toward the basin under the westerly wind and rapidly accumulation of heat may produce an occurrence of very high air temperature at the surface of the basin.

On the other hand, the latent heat flux in the valley surface (here, basin) is greater than that from the mountain surface. As shown in Fig. 7b, latent heat fluxes due to evaporative cooling of the surface are 270 W/m^2 over the ground surfaces of the mountain, which is slightly smaller than 300 W/m^2 over the basin. Below the height of 300m over the ground, convergence of latent heat flux is detected and high gradient of latent heat fluxes are also found along the slope of the mountain and coastal site. As more water vapor can be evaporated in the basin than the mountain area, the air in the basin could be drier than the mountain. So, horizontal transport of moisture can occur from the valley to the top of

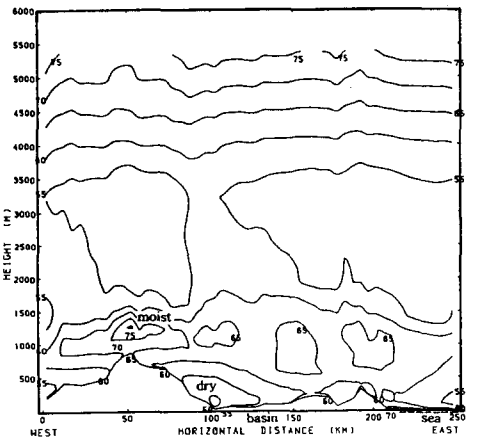

Fig. 8. As shown in Fig. 4a, except for relative humidity (%).

mountain. In the mountainous areas, atmospheric humidity is greater than at the valley or in the basin due to the transport of moisture from the basin to the mountain, but in our case, this transport is small (Fig. 8). Relative humidities (RH) of 65% to 75% over the mountain sides are greater than the RH of 50% in the basin, especially near Taegu city. Thus, the higher relative humidity in the mountain area may be, mainly, due to reduction of evaporation over high mountain surfaces such as relatively smaller latent heat flux than over the basin and slightly horizontal transport of water vapor from the basin to the mountain area. The low relative humidity in the basin is also caused by the accumulation of sensible heat from the mountain to the basin, drying out the moist air on the basin surface.

4.3 Nocturnal thermal high and formation of tropical night

Nighttime air temperature near the ground surface are not much changed with only small different magnitudes of 8^0C to 6^0C such as 31^0C to 33^0C from one during the day (Fig. 9).

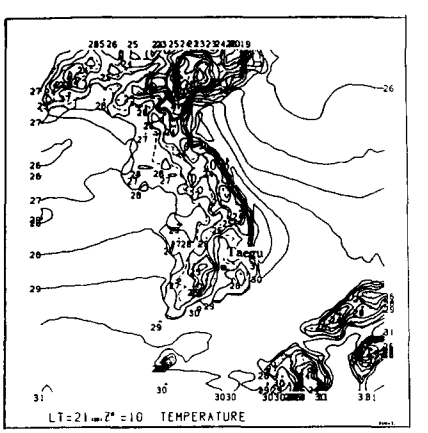

Fig. 9. Horizontal distribution of air temperature (^{0}C) surrounding Korean peninsula in a coarse-mesh domain near Korea at 2100 LST, August 14, 1995.

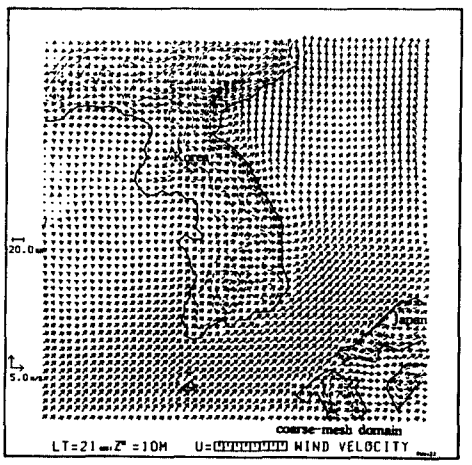

Fig. 10a. As shown in Fig. 9a, except for horizontal wind field (m/s).

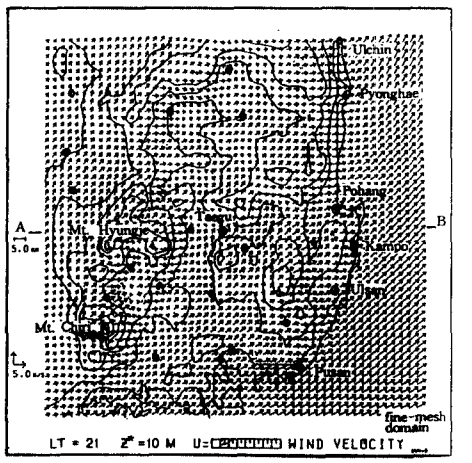

Fig. 10b. Horizontal wind field (m/s) in a fine-mesh domain near Taegu city at 2100 LST, August 14, 1995.

It means that the air near the ground surface continues to be warmed up and the air temperature does not get much lower by nighttime cooling of the ground surface, under no incoming solar radiation after sunset. As nighttime goes on, especially at 2100 LST, westerly and south-westerly flows along the eastern downslope of Mt. Hyungje toward the western inlet of the basin, just near Taegu city are intensified by both synoptic scale westerly wind and land breeze due to the horizontal air temperature difference between over the mountain and the basin surfaces by the ground surface cooling (Fig. 10a and 10b). At this time, the wind speed on the lee side slope of Mt. Hyungje increases to 10 m/s, but in the basin, the nighttime surface wind speed is almost in the same magnitude of 4 m/s as the daytime one (Fig. 11a and 11b).

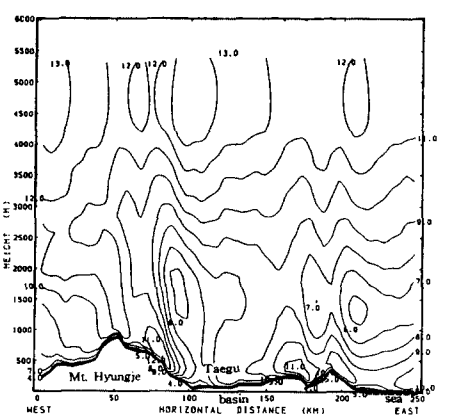

Fig. 11a. Vertical profile of wind (m/s) on a staight cutting line (A-B): Mt. Hyungje (west)-Taegu-Kampo (east) in a fine-mesh domain as shown in Fig. 10b at 2100 LST, August 14, 1995.

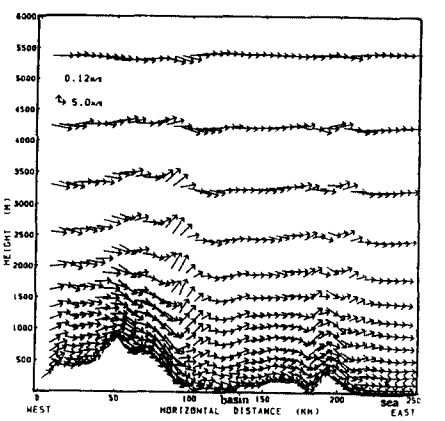

Fig. 11b. As shown in Fig. 11a, except for wind vector (m/s).

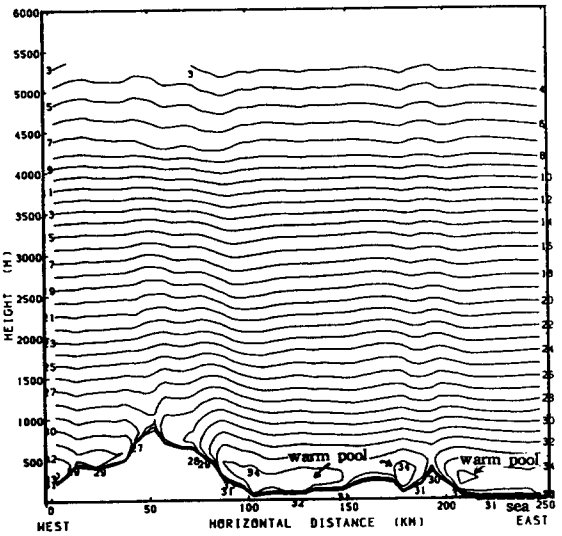

Fig. 12a. As shown in Fig. 11a, except for air temperature (^{0}C).

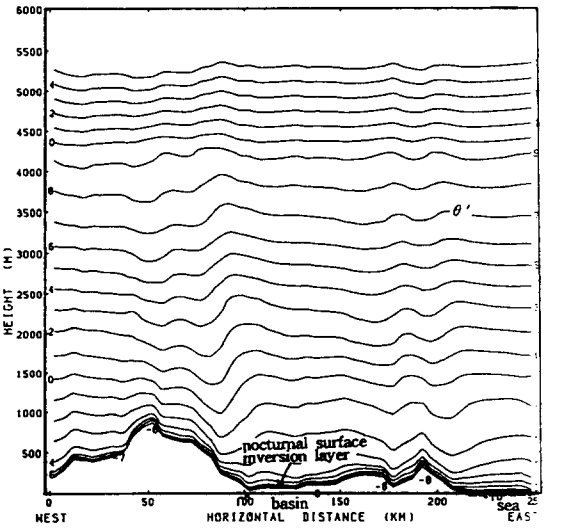

Fig. 12b. As shown in Fig. 11a, except for potential temperature deviation (K).

In Fig. 12a, air temperature near the ground surface of Taegu city is observed with a magnitude of 31^{0}C to 32^{0}C and warm air mass with the temperature of 34^{0}C is isloated over the ground surface of the basin, forming a warm pool. Vertical gradient of potential temperature deviation is very dense near the surafce, which imply the existence of very shallow nocturnal surface inversion layer (NSIL) caused by nighttime radiative cooling and the thickness of the NSIL is within the height of about 150 m over the ground (Fig. 12b). The turbulent diffusion coefficients for momentum and heat are also very small magnitudes of 1 W/m^2 and they are confined to a thin layer just over the surface (Fig. 13a and 13b).

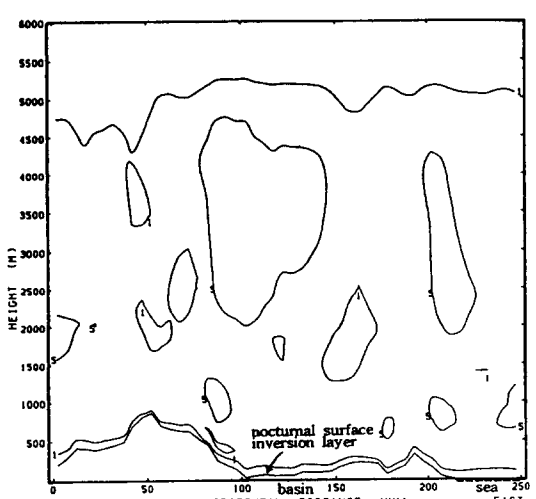

Fig. 13a. As shown in Fig. 11a, except for vertical diffusion coefficient for turbulent momentum (W/m^2).

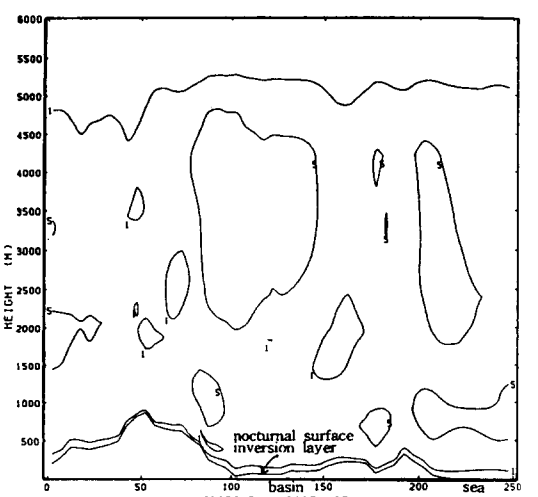

Fig. 13b. As shown in Fig. 11a, except for vertical diffusion coefficient for turbulent heat (W/m^2).

This NSIL is much lower than typical surface inversion layer generated by nighttime surface cooling. As the warm pool produced by the extremely heated air, during the day, is located over the shallow surface inversion and heat from the warm pool is continuously transported into the basin surface, air at the basin surface does not much cool down and continues to keep high temperature through the night, called nocturnal thermal high or tropical night.

This shallow inversion layer is quite different from frequently observed nocturnal surafce inversion layer influenced by the nighttime cooling of the air near the surface of the basin, which Andre and Mahrt (1981) demonstrated before. In part, the tropical night with a high air temperature in the lower atmosphere is similar to a typical nighttime warming of the air produced by adiabatic heating due to the strong downslope flow in the lee side mountain (Choi and Choi, 1997). Since the downslope wind speed along the eastern slope of Mt. Hyungje reaches 11 m/s, adiabatic heating due to descending motion of air parcels makes the increase of temperature along the slope of the mountain and at the valley, even if the wind in the basin still has a moderate speed of 4 m/s. So relative humidity over the eastern slope of the high mountain becomes very low with a magnitude of 45%, due to drying out some of water vapor by adiabatic heating under the strong downslope wind (Fig. 15).

According to Fig. 14a and 14b, sensible heat flux along the eastern slope of Mt. Hyungje

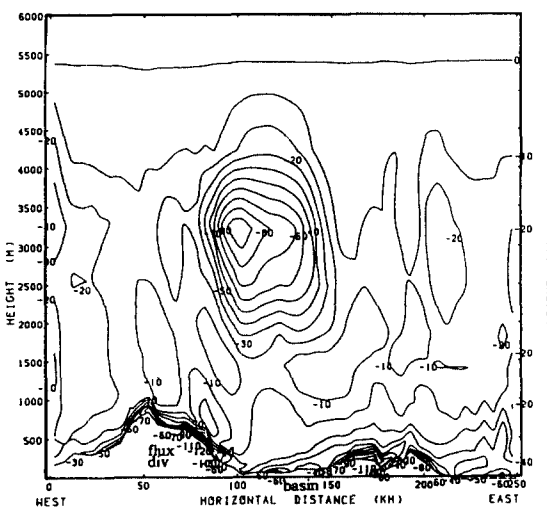

Fig. 14a. As shown in Fig. 11a, except for sensible heat flux (W/m^2).

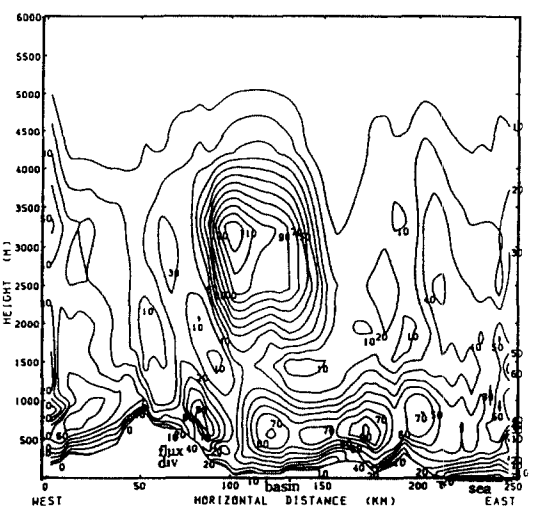

Fig. 14b. As shown in Fig. 11a, except for latent heat flux (W/m^2).

has negative value of -120 W/m^2 which indicates the gain of the heat from the lower atmosphere into the surface, but its flux near the basin is just -60 W/m^2. Divergence of sensible heat flux is greater on the top of the mountain than at the surface of the basin. It appears that the surface in the mountainous area more cools down than that in the basin, and the air temperature near the surface of the basin at night is not much changed from that during daytime, resulting in the persistence of nocturnal warming.

Latent heat flux at the surface of the eastern slope of the mountain is greater than that

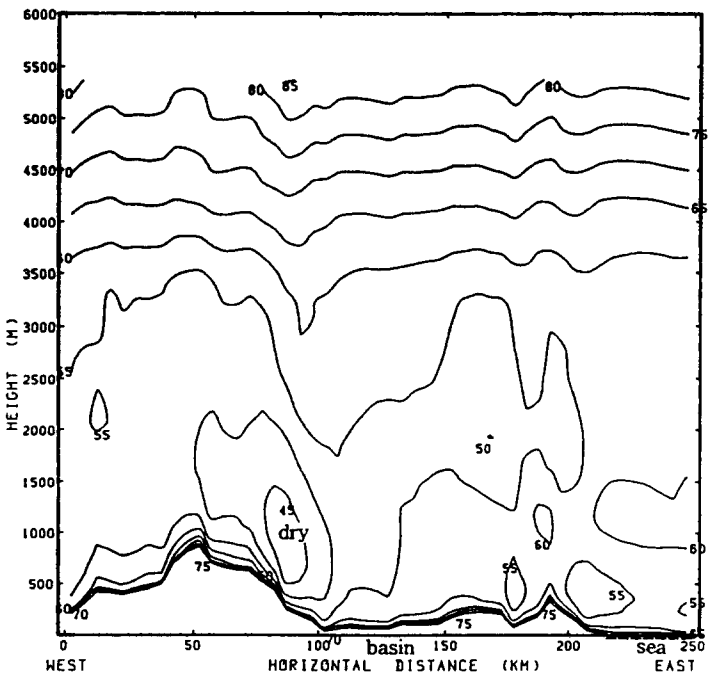

Fig. 15a. As shown in Fig. 11a, except for relative humidity (%).

at the surface of the basin and the maximum latent heat flux in the lower layer occurs below the 500 m height over the ground. Greater divergence of the latent heat flux over the basin than over the mountain can induce high relative humidity of 75% at the surface of the basin and slightly low relative humidity of 65% along the eastern slope of the high mountain, as shown in Fig. 15. As a result, even if the cooling of ground surface take a place at night under the radiative cooling, the air with high moisture under the influence of heat transfer from warm air masses (warm pool) aloft into the ground surface is not much cooled at the surface of the basin, causing the longtime persistence of nocturnal warming, namely, tropical night at Taegu city.

5. Conclusion

During the day, Taegu city in an inland basin, which is under the influence of south-westerly winds, is not directly affected by advection of moisture or heat induced by common sea breeze circulation from coastal sea in the east toward inland in the west. However, the significance of sensible heat flux convergence occurs in the lower atmosphere over the top of the mountain, enhancing warming up of the layer. Since the difference between sensible heat fluxes over the mountain and basin induces horizontal transport of sensible heat flux toward the lower atmosphere over the basin and the downward motion of horizontally transported sensible heat flux accumulates some amounts of sensible heats over

the basin, more accumulation of sensible heat flux in basin than over mountainous area causes an occurrence of the highest air temperature of 39.5^{0}C at Taegu city. At this time, convergence of latent heat flux along the slope of the mountain is smaller than that at the surface of the basin and more water vapor is evaporated in the basin than the mountain area. Through horizontal transport of moisture from the valley or the basin to the top of mountain, the air at the surface of the basin is drier than the mountain.

At night, divergence of sensible heat flux on the top of the mountain, which is greater than that in the surface of the basin, may induce greater cooling of the air at the mountain surface than the basin surface. High relative humidity of 75% is found at the basin surface and slightly low relative humidity of 65% is along the eastern slope of the high mountain. Thus, the air temperature near the surface of the basin with high moisture in the evening becomes not much changed from that during the day, resulting in the persistence of nocturnal warming. Furthermore, as a warm pool produced by the extremely heated air, during the day, is located over the shallow nocturnal surface inversion, some amounts of heat from the warm pool is continuously tranported into the surface of the basin, causing warming up the air near the ground surface and forming tropical night at Taegu city.

6. Acknowledgement

The authors wish to thank Mr. S. Takahashi, JMA, for developing computer programs essential to this work and to Dr. Junji Sato and Dr. T. Hanafusa of Meteorological Research Institute for the use of HITACH super computer. National Fisheries Research and Development Agency of Korea provided the reanalyzed SST data from NOAA satellite image picture. Finally, we would like to thank the reviewers for their helpful comments and suggestions. This research was supported, in part, by the Ministry of Environment in 1996, under grant for "Development of forecasting techniques on regional climate change-G7 research project" and by Korea Science and Engineering Foundation, the Ministry of Science and Technology in 1997 for "Long-range transport processes with dry and wet deposition of sulfure" through "Training program of senior scientific researcher in Japan".

References

Andre, J. C. and L. Mahrt, The nocturnal surface inversion and influence of clear-air radiative cooling, *J. Atmos. Sci., 39,* 864-878, 1982.

Arya, A. P, *Introduction to micrometeorology,* Academic Press, 307pp, 1988.

Boer, G. J., N. A. McFarlane and R. Laprise, The climatology of Candian climate center general circulation model as obtained from a five year simulation, *Atmos. Ocean., 22,* 430-473, 1984.

Broast, R. A. and J. C. Wyngaard, A model study of the srably-stratified planetary boundary layer, *J. Atmos. Sci., 35,* 1427-1440, 1978.

Choi, H. and J. Choi, Numerical simulation on mountain and sea breeze effects influenced upon long-range transport of total suspended particles during the yellow sandy event, *Measurement and modelling in environmental pollution, Comp. Mechan. Pub.,* 201-210, 1997.

Choi, H., J. Choi, S. Takahashi and T. Yoshikawa, Three dimensional numerical modelling on the development of thermal and mechanical internal boundary layers in the Cheju island, *J. Korean Meteor. Soc., 32,* 1-16, 1996..

Deardorff, J. W., Efficient prediction of ground surface temperature and moisture with inclusion of a layer of vegetation, *Geophys. Res., 38,* 659-661, 1978.

Hsu, S. A., Research in the coastal meteorology: basic and applied, *Proceeding of 2nd Conference on Coastal Meteorology,* Los Angles, Amer. Meteor. Soc., 1-7, 1980.

Hsu, S. A., *Coastal Meteorology,* Academic Press, 260pp, 1988.

Kimura, F. and S. Arakawa, A numerical experiment of the nocturnal low level jet over the Kanto plain, *J. Meteor. Soc. Japan, 61,* 848-861, 1983.

Kimura, F. and S. Takahashi, The effects of land-use and anthropogenic heating on the surface temperature in the Tokyo metropolitan area: numerical experiment, *Atmospheric Envir., 25,* 155-164, 1991.

Klemp, J. B. and D. R. Durran, An upper condition permitting internal gravity wave radiation in numerical mesoscale models, *Mon. Wea. Rev., 111,* 430-440, 1983.

Kondo, J. T., Kuwagata and S. Haginoya, Heat budget analysis of nocturnal cooling and daytime heating in a basin, *J. Atmos. Sci., 46,* 2917-2933, 1989.

Kuwagata, T. and M. Sumioka, N. Masuko and j. Kondo, The daytime PBL heating process over complex terrain in central Japan under fair and calm weather conditions. Part I: Meso-scale circulation and the PBL heating rate, *J. Meteor. Soc., Japan, 68,* 625-638, 1990.

McPherson, R. D., A numerical study of the effect of a coastal irregularity on the sea breeze, *J. Appl. Meteor., 9,* 767-777, 1970.

Mellor, G. L. and T. Yamada, A hierachy of turbulence closure models of planetary boundary layers, *J. Atmos. Soc., 31,* 1791-1805, 1974.

NFRDA, *Analyzed NOAA satellite picture on the sea surface temperature in the East Sea (Japan Sea),* National Fisheries Research and Development Agency, 1994.

Orlanski, I., A simple boundary condition for unbounded hyperbolic flows, *J. Comp. Phys., 21,* 251-269, 1976.

Palmer, T. N., G. J. Smith and R. Swinbank, Alleviation of a systematic westerly bias in general circulation and NWP models through and orographic gravity wave drag parameterization, *Q. J. R. Meteor. Soc., 112,* 1001-1039, 1986.

Plate, E. J., *Aerodynamic characteristics of atmospheric boundary layers,* 190pp, U. S. Atmospheric Energy Commission, 1971.

Raynor, G. S., S. SethuRaman and R. M. Brown, Formation and characteristics of coastal internal boundary layer during onshore flows, *Boundary Layer Meteor., 16,* 4587-514, 1979.

Satomura, T. and P. Bougeault, Orographic wave drag during PYREX experiment, *Proceeding of Spring Meeting of the Meteorological Society of Japan,* Tsukuba, 1-282, 1992.

Segal, M., C. H. Yu, R. W. Arritt and R. A. Pielke, On the impact of valley/ridge thermally induced circulations on regional pollutant transport, *Atmos. Environ., 22,* 471-486, 1988.

SethuRaman, S., Observation of the bounadry layer wind structure near land-sea interface, *Proceeding of 1st International Conference on Meteorology and Air/Sea Interaction of the coastal Zone,* Hague, Amer. Meteor. Soc., 4-7, 1982.

Whiteman, C. D., Observations of thermally developed wind system in mountainous terrain, *Atmospheric Processes over complex terrain, Meteor. Monogr.,* No. 40, Amer. Meteor. Soc., 5-42, 1990.

Yamada, T., Simulation of nocturnal drainage flows by a q^2-l turbulence closure model, *J. Atmos. Sci., 40,* 91-106, 1983.

Yamada, T. and G. L. Mellor, A numerical simulation of the BOMEX data using a turbulence closure model coupled with ensemble cloud relations, *Q. J. R. Meteor. Soc., 105,* 95-944, 1983.